Applied Catalysis B: Environmental 95 (2010) 208–216

Contents lists available at ScienceDirect

Applied Catalysis B: Environmental

journal homepage: www.elsevier.com/locate/apcatb

Promoting behaviors of alkali compounds in low temperature methanol synthesis over copper-based catalyst

Baoshan Hu [1], Kaoru Fujimoto *

Department of Chemical Processes and Environments, Faculty of Environmental Engineering, University of Kitakyushu, 1-1, Hibikino, Wakamatsu, Kitakyushu 808-0135, Japan

ARTICLE INFO

Article history:
Received 5 September 2009
Received in revised form 6 December 2009
Accepted 3 January 2010
Available online 11 January 2010

Keywords:
Methanol synthesis
Low temperature
Sodium compound
Cu/MgO catalyst
Active site

ABSTRACT

Hybrid catalyst systems comprised of Na compounds (HCOONa, NaOH, Na_2CO_3 and $NaHCO_3$) and Cu/MgO catalysts have contributed to a novel high-performance methanol synthesis in ethanol solvent from syngas ($CO/H_2 = 1/2$) at a low temperature of 433 K and 5 MPa. It is found that Na_2CO_3 dopant is more beneficial to enhance hydrogenolysis ability of Cu/MgO catalyst than NaOH and HCOONa. Whereas, all the starting Na compounds in ethanol solvent are reversibly converted to HCOONa in alcohol solvent by *ex situ* observations, revealing that formate alone is the essential species in the catalytic circle. The results unambiguously elucidate that the essence of alkali component in promoting the low temperature methanol synthesis is virtually attributed to the formation of highly reactive alkali-participated active site. It is also proposed that solid Cu/MgO catalyst should play binary roles in successive carbonylation and hydrogenolysis reactions.

1. Introduction

The production of methanol has been commercialized for many decades. At present, over 75% of the world's production has been made through gas phase process. The process using typical $Cu/Zn/Al_2O_3$ or, less preferably, $Cu/Zn/Cr_2O_3$ with natural gas-, coal-derived syngas has been operating under severe conditions (220–300 °C, 5–8 MPa) [1,2]. Most presently, sulfur-tolerant and CO_2/H_2-directed processes for methanol synthesis have evoked some researchers' interest [3,4]. However, one-pass conversion of syngas to methanol in current commercial plants is limited at a lower level of about 25% by exothermic equilibrium. Especially, photochemical routes have generated the feasibility for synthesis of methanol using water-soluble zinc porphyrin in aqueous media with [5], which might open up an attractive path for methanol synthesis.

A liquid phase methanol synthesis technology was developed by US Department of Energy (DOE) to overcome the exothermic problem of reaction [6]. This proved the viability of slurry bed concept, but operation temperatures remained high. Later, Brookhaven National Laboratory of USA (BNL) evolved a liquid phase process at 373–403 K and 1.0–5.0 MPa, using strong base catalyst composed of NaH, alcohol and $M(Ac)_2$ (M = Ni, Pd and Co) and pure syngas ($CO + H_2$) [7]. Also, strongly basic catalyst would be deactivated soon by a trace amount of carbon dioxide and water in the feed gas.

An alternative method of methanol synthesis from pure CO and H_2 has been widely studied, where carbonylation of methanol and hydrogenation of the formed methyl formate are considered as the two main steps of the reactions [8–11]. The overall reaction can be carried out in a slurry reactor with consequent good heat transfer rates and with a rate of reaction at low catalyst loadings comparable with that in the commercial synthesis. The only significant products are methanol and methyl formate, which can be separated easily. Ohyama, Aika and Wender realized this synthesis in liquid phase using a mixed catalyst composed of alkali metal alkoxide and copper- or nickel-based compounds under the mild conditions of 373–453 K and 5.0–6.5 MPa. Their methods gave high methanol synthesis rates and high one-pass CO conversions [8–11]. The extremely mild conditions of LTMS were postulated as being due chiefly to the more easy reduction of the activated carbon–oxygen bond in methyl formate as compared with that of CO coordinated to a metal.

$$CO + CH_3OH = HCOOCH_3 \qquad RONa \qquad (1)$$

$$HCOOCH_3 + 2H_2 = 2CH_3OH \qquad Solid\ Cat. \qquad (2)$$

$$\text{Net} \qquad CO + 2H_2 = CH_3OH \qquad (3)$$

(However, similar to BNL process, the used alkoxide catalysts reacted facilely with H_2O or CO_2 to form alkali formates (e.g.

* Corresponding author.
E-mail address: fujimoto@env.kitakyu-u.ac.jp (K. Fujimoto).
[1] Present address: Institute for Materials Chemistry and Engineering, Kyushu University, and Graduate School of Engineering Sciences, Kyushu University, Kasuga, Fukuoka 816-8580, Japan.

0926-3373/$ – see front matter © 2010 Elsevier B.V. All rights reserved.
doi:10.1016/j.apcatb.2010.01.001

HCOONa) and alkali methyl carbonates (e.g. $NaOCOOCH_3$), respectively [9]. Particularly, conversion of alkoxide into alkali formate was viewed as one of reasons for the deactivation [12]. Afterwards, Palekar et al. [8] found that the used Cu-based catalyst could regenerate the deactivated alkoxide catalyst by catalyzing the hydrogenolysis of alkali formate and alkali methyl carbonates and also removed water by WGS reaction, and that alkali formate was as active as alkali methoxide in the concurrent synthesis. These studies put the catalytic functions and reaction mechanisms of alkoxide and alkali salts into penetrating controversies in the LTMS. Therefore, some researchers have thrown their insights into catalytic systems in the absence of alkali promoter for LTMS, although it will usually be at the expense of not so high activity. In particular, it has been claimed that the utilization of alcohol solvent remarkably lowered the reaction temperature of methanol synthesis and realized the LTMS from syngas containing carbon dioxide over Cu/ZnO catalysts [13–16]. Herein, ROH is recognized as a catalytic solvent since it is not only a reaction medium but also participates in the reaction of methanol synthesis catalytically [14].

To date, applications of alkali dopants in enhancing the methanol synthesis rates over metal/oxide heterogeneous catalysts other than resorting to higher noble metal loadings have been investigated. Alkali dopant has been demonstrated to work through three typical ways: electrostatic force; participating in the charge transfer; and changing the bonding of formate to the catalyst surface [17–19]. Klier, Sheffer and King reported the promotion effect of the alkali compounds on copper-based catalysts for direct methanol synthesis [20–22]. Especially in the slurry phase LTMS, some synergic function was experimentally confirmed between alkali methoxide and copper catalyst [9]. However, there are a few systematic reports on the applicability and mutual relationships of other alkali dopants beside alkali methoxide in the slurry LTMS, especially on the real role of alkali promoter.

Recently, we have developed a novel high-performance LTMS in the liquid phase over Cu/MgO solid catalyst, in the presence of alkali formate and ethanol solvent [23], where alkali was quite indispensable for attaining the high activity. As an extended study, this paper will elaborately investigate the promotion effects of several representative Na compounds, including HCOONa, Na_2CO_3, $NaHCO_3$ and NaOH, as well as the inter-transformation behaviors of these species, with the aim of emphasizing the essence of alkali dopant in the slurry phase LTMS.

2. Experimental

2.1. Catalyst preparation

The used Cu/MgO–Na catalyst was prepared by the conventional co-precipitation and impregnation methods. In brief, an aqueous solution of copper nitrate (0.086 mol/l) and magnesium nitrate (0.086 mol/l) and an aqueous solution of sodium carbonate were simultaneously added at 333 K and a constant pH value of 10 into a well-stirred thermo-stated container. The obtained precipitate was filtrated and washed with distilled water, followed by drying at 393 K for 6 h and calcination in air at 623 K for 1 h. The resulting powder was defined as the basic Cu/MgO catalyst.

For Na-impregnated catalysts, the Cu/MgO catalyst was impregnated with an aqueous solution of Na_2CO_3, HCOONa and NaOH, respectively, as a nominal composition of 9 wt% Na material. After impregnation, the obtained samples were also dried at 393 K for 6 h and calcinated at 623 K for 1 h to form Cu/MgO–Na_2CO_3 (in air ambience; this was the standard case and was abbreviated as Cu/MgO–Na in the text), Cu/MgO–HCOONa (in N_2 ambience) and Cu/MgO–NaOH (in N_2 ambience), respectively. Finally, all these catalysts need to be reduced in a stream of H_2 at 523 K (or 623 K) for 1 h before their activity evaluations.

2.2. Catalyst characterizations

The phases of copper catalyst were characterized by X-ray diffraction (XRD) with an RINT 2000 System (Rigaku) diffraction meter using Cu Kα radiation. Patterns were recorded from 15° to 80° (2θ) at 40 kV and 20 mA. Crystalline size (D) of Cu metal was calculated by the XRD line width of the strongest peak Cu (1 1 1) ($2\theta = 43.4°$), using the Debye–Scherrer equation.

The surface morphology of catalyst was observed by scanning electron microscopy (SEM; Hitachi S-4800). The specific surface area of catalyst was determined by BET method and pore structure properties of catalyst was determined by BJH method, using an Autosorb-1 Quantachrome apparatus with nitrogen as adsorbate at 77.3 K after a pretreatment of vacuum degassing at 423 K.

The uptakes of H_2- and CO-chemisorptions were also measured by an extrapolation method of chemisorption isotherms on an Autosorb-1 Quantachrome apparatus. For the fresh Cu/MgO and Cu/MgO–Na catalysts, *in situ* reduction process by H_2 identical to that in the activity evaluation was conducted prior to H_2- and CO-chemisorptions; the chemisorption temperature was the same as the reaction temperature of 433 K.

FT-IR with a spectrum GX 2000R (Shimadzu) was used to *ex situ* investigate sodium compounds dissolved in liquid phase. The dissolved salt samples were attained by vaporizing the liquid products, such as methanol, ethanol, and so on, with N_2 protection at 313 K for 12 h.

2.3. Reaction procedures

Alkali compound (10 mmol, Kanto Chemical Co., Inc.) was added to a flow type semi-batch autoclave reactor with an inner volume of 85 ml [23], and then the reduced catalyst (2.0 g) and high purity ethanol (30 ml, Kanto Chemical Co., Inc.) were poured into the reactor inside a vacuum glove box (Miwa Seisakusho Co., Ltd.). After flowing N_2 to keep air out of retention volume of the reactor, the system was purged with feed gas till to reaction pressure level; then, temperature was increased to 433 K within 20 min. The composition of standard feed gas was H_2/CO/Ar = 64.56/32.4/3.04. The stirring speed was 1660 rpm for attaining a uniform reaction phase and remaining the liquid phase in the reactor under the reaction temperature and pressure [24]. All products were analyzed by two gas chromatographs, in which GC-8A/TCD (Shimadzu) was used for gas products and GC353/FID (GL Science) was used for liquid products. Considering the retention volume, conversion of syngas ($CO/2H_2$) was calculated by Eq. (4). The formation rates STY (mol/kg-cat. h), as well as the selectivities of methanol and other liquid components, were calculated by using 1-propanol as an external standard:

$$\text{CO-conv.}\% = \frac{F_{\text{in,CO}} - F_{\text{out,CO}}}{F_{\text{in,CO}}} \times 100\% \quad (4)$$

Herein, $F_{\text{in, syngas}}$ ($F_{\text{out, syngas}}$) is the molar flowrate of syngas in the inlet (outlet) gas phase.

3. Results

3.1. Impregnation of Na dopant on Cu/MgO catalyst

3.1.1. Doping effect of Na associated anion

Our foregoing result has clarified that Na cation exhibits the most optimizing coordination with Cu/MgO substrate in the X formate/(Cu/MgO–X_2CO_3) (X = Na^+, K^+, Rb^+ and Li^+) catalyst system

Table 1
Reaction performances of Cu-based catalysts for LTMS in slurry phase[a].

Catalyst	Conversion (%)[b]	STY (mol/kg-cat. h)[c]	Selectivity (C—mol%)						
			Methanol	MeF	EtF	CO_2	CH_4	Methyl acetate	Dimethyl carbonate
Cu/MgO	7.2	1.6	57.5	0.0	1.2	2.7	0.0	0.0	38.6
Cu/MgO–HCOONa	38.4	12.9	91.7	1.3	0.3	0.3	0.1	2.8	3.5
Cu/MgO–Na_2CO3	40.1	17.4	93.3	1.9	0.3	0.2	0.1	2.4	1.8
Cu/MgO–NaOH	19.3	8.5	89.9	0.0	0.0	0.8	0.0	3.1	6.2

[a] Reaction conditions: Cu/MgO–Na catalyst, 2.0 g; HCOONa, 10 mmol; syngas flowrate, 90 ml/min; ethanol, 30 ml; 433 K, 5 MPa; 24 h.
[b] The data are the CO conversions at stable state of 24th reaction hour.
[c] The data are the average values over the total reaction time of 24 h.

for methanol synthesis [25]. Successively, it is necessary to study the effect of different Na-associated anion precursors as the impregnators of Cu/MgO catalyst. Table 1 compares the reaction performances of Cu/MgO catalysts impregnated individually with Na_2CO_3, HCOONa and NaOH.

It is obvious from the data that the impregnation of Na dopant greatly enhances the reaction activity of Cu/MgO catalyst, and thus the basic function of alkali probably plays a dominant role in the concerted reaction mechanism, as was early implied in the case of Cu and Zn bifunctional catalyst for methanol synthesis [19]. In contrast, a standard Na_2CO_3 case gives highest promotion to the methanol formation rate (STY) of Cu/MgO catalyst; HCOONa enhances the STY of Cu/MgO catalyst to a little lower extent, with unexpected low selectivity to methyl formate (MeF). Noticeably, the CO conversions for the two catalysts change largely with the reaction time, so the data of CO conversions at the 24th reaction hour shown here are inconsistent with the data of the accumulated STYs during the total reaction time. Whereas, NaOH impregnation shows quite low activity; meanwhile, the selectivities to methyl formate and ethyl formate (EtF) are zero, which can be ascribed to highly selectable by-pass reactions manufacturing methyl acetate and dimethyl carbonate (DMC), shown in Table 1. The series of results intriguingly indicate that alkali dopant promotes the process more efficiently in the form of carbonate. An adducible finding by Campbell proposed that Cs dopant combined with carbonate acted as a role of O mediator in the water–gas shift reaction over Cu (1 1 0) [26].

X-ray powder diffraction (XRD) traces of these catalysts after H_2 reduction show well defined crystalline pattern of Cu metal (2θ = 43.4°, 50.5° and 74.2°), as are plotted in Fig. 1. For all the Na-impregnated copper magnesium catalysts, a novel phase $Na_2Mg(CO_3)_2$ named eitelite is detected, which has the lattice of hexagonal cell [27] and is identified by XRD patterns with code 24-1227 of PDF database. This phase is contrastively absent in Cu/MgO catalyst. Moreover, the trace of Cu/MgO–Na (hereafter, referring as Na_2CO_3 impregnation described in Section 2.1) appears the $Na_2Mg(CO_3)_2$ phase at a smaller diffraction angle of 2θ = 34.4° than those at 2θ = 36.3° of Cu/MgO–HCOONa and Cu/MgO–NaOH, showing the abundance of crystalline structure with bigger interlayer distance. It reflects that anion precursor determines the structure of atomic lattice in the resultant $Na_2Mg(CO_3)_2$ which works as a substrate of metallic Cu phase; however, to understand the relationship between the structure of $Na_2Mg(CO_3)_2$ atomic lattice and the activity of alkali impregnated Cu/MgO catalyst need further evidence.

3.1.2. Effect of Na_2CO_3 loadings

Fig. 2 shows the activities of Cu/MgO–Na catalysts with different loadings of Na_2CO_3 impregnation. From the data, rate of methanol synthesis is positively dependent on the loading of Na_2CO_3 up to a peak point at 9 wt% Na_2CO_3 and then descends. It is meanwhile shown that, in the absence of Na_2CO_3, concentration of methyl formate is nearly zero although methanol product is abundant in the liquid phase; while, ethyl formate keeps a higher concentration. Hereafter, an increase of Na_2CO_3 loading results in the increasing concentrations of methyl formate and ethyl formate. At lower Na_2CO_3 loadings, they are favorable to the methanol formation rates, since a sharp increase in methanol formation rate is seen in the range of 0–5 wt% Na_2CO_3 loading; at higher loadings, however, the whole reaction of methanol synthesis decelerates in spite of higher concentrations of alkyl formates produced simultaneously. One possible explanation is that the excessive alkali covers some part of hydrogenolysis sites on the surface of Cu/MgO catalyst [24]. These results suggest that the Na_2CO_3

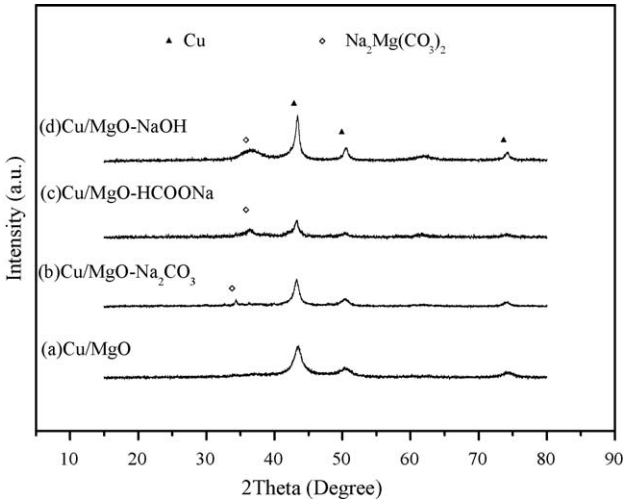

Fig. 1. XRD patterns for various reduced copper magnesium catalysts impregnated by different Na precursors. (a) Cu/MgO; (b) Cu/MgO with Na_2CO_3 impregnation; (c) Cu/MgO with HCOONa impregnation; (d) Cu/MgO with NaOH impregnation.

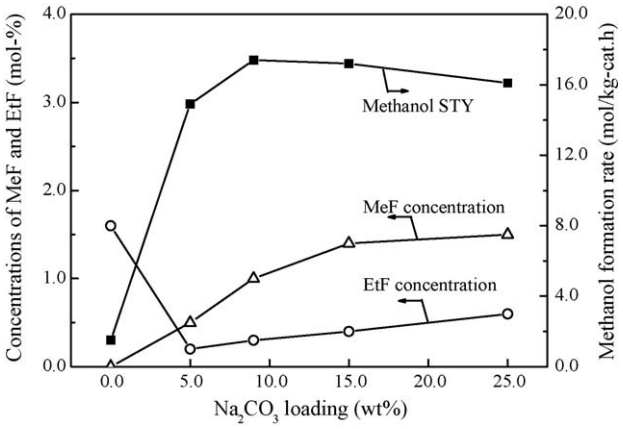

Fig. 2. Reaction performance of Cu/MgO–Na catalyst as a function of Na_2CO_3 loading in the presence of soluble HCOONa. Reaction conditions: Cu/MgO–Na catalyst, 2.0 g; HCOONa, 10 mmol; syngas flowrate, 90 ml/min; ethanol, 30 ml; 433 K, 5 MPa; 24 h.

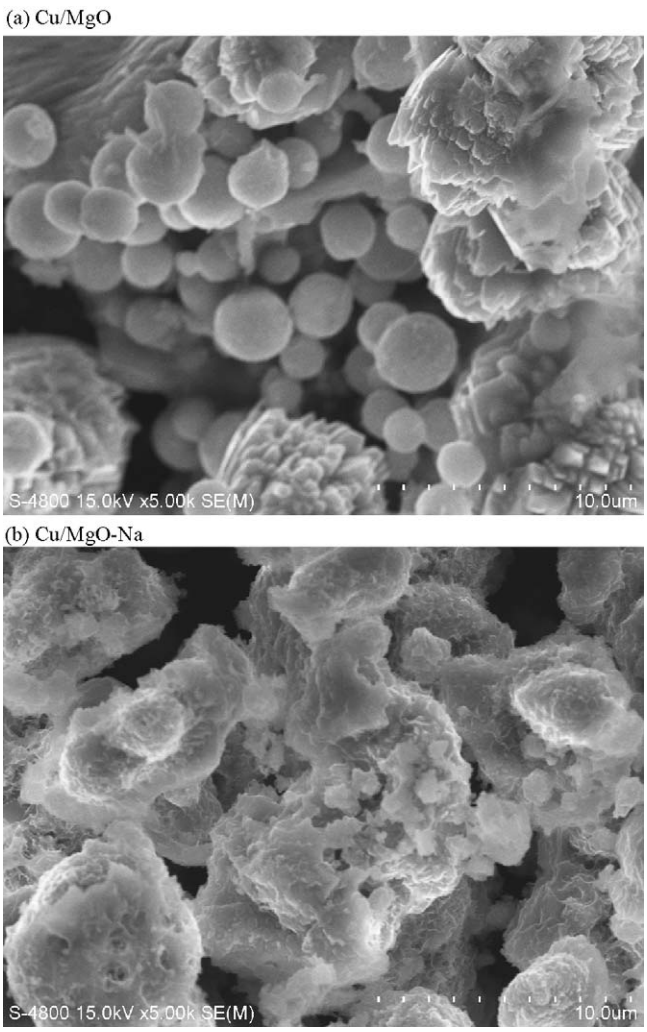

Fig. 3. SEM images of Cu/MgO and Cu/MgO–Na catalysts.

impregnation reinforces the hydrogenolysis ability of Cu/MgO rather than the possible carbonylation function of Na_2CO_3, because concentrations of methyl formate and ethyl formate working as intermediates [15,23,25] are competitively determined by steps (1) and (2).

3.1.3. Characterization of Cu/MgO and Cu/MgO–Na catalysts

First, SEM images of fresh Cu/MgO and Cu/MgO–Na(9 wt%) catalysts are displayed in Fig. 3. The distinctive morphologic features appear that some spheroidal particles which are probably CuO identified by XRD patterns [23] are adhered onto bulky substrate in Cu/MgO catalyst, the particle size is mostly in the range of 1–3 μm; for Cu/MgO–Na catalyst, these particles are encapsulated together with some bulky-lamellar crystals which is ascribed to post-impregnated Na_2CO_3 or $Na_2Mg(CO_3)_2$ mentioned above.

The pore structure properties of fresh Cu/MgO and Cu/MgO–Na catalysts from N_2-physisorption isotherms, as well as the H_2- and CO-chemisorption abilities after their reductions by H_2 flow, are showed in Table 2. Na impregnation greatly depresses the BET surface and pore size of Cu/MgO catalyst, which is consistent with the above SEM images.

In LTMS process, high H_2 adsorption intensity of solid hydrogenolysis catalyst is favorable to the H_2 dissociation adsorption. Whereas, the appropriate adsorption of carbonyl group in alkyl formate molecule by copper-based catalyst is favorable to its activation and successive hydrogenolysis [28]; however, CO is conversably poisonous to copper-based catalyst [29–31]. Consequently, the actual rate of methanol synthesis relies on the relative magnitude of these effects very evidently. From Table 2, for Cu/MgO and Cu/MgO–Na both reduced at 523 K, the impregnation of Na_2CO_3 greatly diminishes the CO uptake of Cu/MgO, showing that the adsorbed amount of carbonyl group in alkyl formate molecule does not determine the ultimate activity. This result is in accordance with our previous study where not hydrogenoloysis but carbonylation was a rate-limiting step for the LTMS [24]. It is noted that the crystalline size ($D_{1\,1\,1}$) of Cu^0, as well as the H_2 uptake, do not change largely by Na impregnation.

3.1.4. Role of Na impregnation

To further verify whether the impregnation of Na_2CO_3 is indispensable for a highly active LTMS, we raise the reduction temperature of Cu/MgO catalyst from 523 to 623 K and then perform an activity evaluation run. From Table 2, high reduction temperature at 623 K increases the H_2 uptakes significantly, which might be attributed to an enhanced interaction between Cu and MgO support as mentioned above [26], or deep reduction of copper phase embedded in MgO or $Na_2Mg(CO_3)_2$ lattices. It is noteworthy in Fig. 4 that, Cu/MgO (623) catalyst exhibits the gradually elevating CO conversion versus reaction time, differently from that reduced at a low reduction temperature of 523 K, and then undergoes the similar tendency of activity drop and methanol selectivity above 90% with the standard Cu/MgO–Na catalyst after 5 h reaction. We conclude that the enhanced activity should be ascribed to the increase of carbonylation reaction rates resulted from the deep reduction of Cu/MgO catalyst, because carbonylation reaction was rate-limiting step [24]. As a consequence, the occurrence of an induction period pronouncedly indicates that the reaction rate is controlled by solid surface reaction on Cu/MgO catalyst, as was stated previously [25], and thus that the massive carbonylation reaction has fulfilled on the catalyst surface. Hence, the induction period can be interpreted as a time when the total active sites are completely accumulated to run reaction at an appreciable rate. In general, the change of intrinsic structure of Cu/

Table 2
Textural structure properties of Cu/MgO and Cu/MgO–Na catalysts.

Catalysts	Pore size (nm)[a]	BET (m^2/g)[b]	Reduction temp. (K)[c]	Crystalline size (D) (nm)[d]	Uptake (μmol/g)[e]	
					CO	H_2
Cu/MgO	90.4	88.6	523	10.8	46.0	119
			623	14.1	58.6	197
Cu/MgO–Na	20.4	32.1	523	11.2	28.4	108

[a] Determined by BJH method with N_2 as adsorbate.
[b] Determined by BET method with N_2 as adsorbate.
[c] The pre-reduction temperatures of copper catalyst by H_2 flow.
[d] Calculated by XRD line width of the strongest peak Cu (1 1 1) ($2\theta = 43.4^\circ$), using Debye–Scherrer equation.
[e] Determined by extrapolation of H_2- and CO-chemisorption isothermals described in the text.

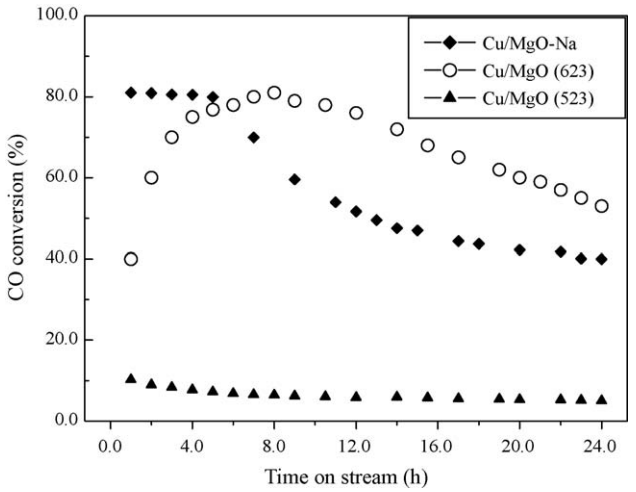

Fig. 4. Activity plots of Cu/MgO and Cu/MgO–Na catalysts versus time on stream. Cu/MgO (523) and Cu/MgO (623) represent that the reduction temperature of Cu/MgO catalyst is 523 and 623 K, respectively. Reaction conditions: copper catalyst, 2 g; HCOONa, 10 mmol; ethanol, 30 ml; 433 K, 5.0 MPa.

MgO due to high reduction temperature is believed to promote the activation of catalyst itself and accomplish the formation of total active species. This mode of activation is probably resulted from a general feature of metallic Cu-support relations extensively supported by many groups [32–36], and/or is ascribed to enhanced strain on the metallic Cu due to the interaction with supporter [37]. As a comparative consequence, it is inferred that existence of alkali dopant might facilitate the catalyst reduction or enhance the interaction between Cu and support, and further strengthen the activation of Cu/MgO even at the low reduction temperature for the catalytic process.

3.2. Promotion effect of Na dopants in the ethanol solvent

3.2.1. Reaction performances

Na_2CO_3, $NaHCO_3$ and NaOH are tested for the possibilities of use as promoters in ethanol solvent, reaction performances of every corresponding catalytic system over Cu/MgO–Na are shown in Fig. 5 and Table 3. With the time on stream, Na_2CO_3 gradually elevates the reaction activity to a steady state level; $NaHCO_3$ enhances the activity quickly up to a stable level which is slightly higher than that of alone Cu/MgO–Na. It means that $NaHCO_3$ has little promotion function. When NaOH is used, CO conversion slowly increases and then follows a similar tail to that of HCOONa. In addition, it is seen from Table 3 that the sorts of main by-products are same, suggesting that in all the activation procedures the catalytically active sites are same and/or can convert reversibly.

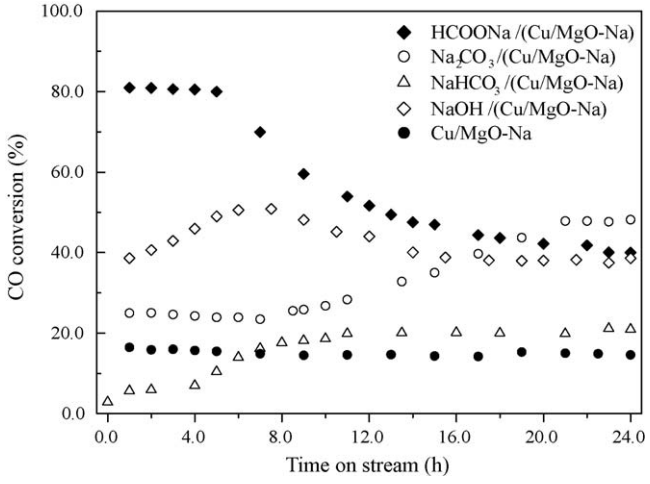

Fig. 5. Reaction activities of Cu/MgO–Na catalyst systems with different Na compounds in ethanol solvent. Reaction conditions: Cu/MgO–Na catalyst, 2.0 g; HCOONa, Na_2CO_3, $NaHCO_3$, NaOH, 10 mmol; syngas flowrate, 90 ml/min; ethanol, 30 ml; 433 K, 5 MPa.

Table 3
Influence of various Na compounds in ethanol solvent on reaction performances over Cu/MgO–Na catalyst[a].

Yield of product (%)	Na compounds in ethanol solvent			
	HCOONa	Na_2CO_3	$NaHCO_3$	NaOH
CH_3OH	48.10	28.70	12.30	44.60
CO_2	0.12	0.07	0.49	0.13
CH_4	0.04	0.00	0.13	0.03
MeF	0.96	0.53	1.15	0.37
EtF	0.14	0.36	0.66	0.16
DMC	0.95	0.16	1.13	0.41
Methyl acetate	1.21	0.96	1.17	0.37

[a] Reaction conditions: Cu/MgO–Na catalyst, 2.0 g; HCOONa, Na_2CO_3, $NaHCO_3$, NaOH, 10 mmol; syngas flowrate, 90 ml/min; solvent, ethanol, 30 ml; 433 K, 5 MPa; 24 h.

3.2.2. Ex situ FT-IR spectra of Na-associated species in the solvent

FT-IR spectra of components dissolved in liquid phase before and after reactions are measured to investigate the consumption and transformation of these Na-associated anions during reaction, as shown in Fig. 6. According to our FT-IR measurement of pure materials and literatures [38–41], the bands at around 1600 and 1360 cm^{-1} are antisymmetric and symmetric stretching vibrations of carbon–oxygen bonds in $HCOO^-$ group, respectively; the bands at around 1460 cm^{-1} is the label band of CO_3^{2-} species; the bands at around 1660, 1620, 1400 and 1300 cm^{-1} are the label bands of HCO_3^- species.

It is found from Fig. 6(a) that, besides the added HCOONa (1600 and 1360 cm^{-1}), some amount of Na_2CO_3 (1460 cm^{-1}) derived from solid Cu/MgO–Na catalyst is dissolved into ethanol solvent under high pressure syngas before reaction in the HCOONa/(Cu/MgO–Na)/ethanol reaction system. We conclude that CO_3^{2-} will be contained in the solution before the reaction of methanol synthesis in all the present cases as soon as the Cu/MgO–Na catalyst is used. Based on this conclusion, all the analysis results for the appeared bands and their attributions before and after reactions are summarized in Table 4. After reaction, the weak band at 1380 cm^{-1} might come from CH_3ONa. Besides, $NaHCO_3$ is deduced by the observable peaks at 1420 and 1310 cm^{-1} which also appear in the $NaHCO_3$/(Cu/MgO–Na)/ethanol reaction system after catalysis. It is noted that the main peaks of HCO_3^- at around 1660 and 1620 cm^{-1} might be overlapped by the peak of $HCOO^-$ at around 1600 cm^{-1} because of the relatively small fraction of $NaHCO_3$ in the obtained sample. Reasonably, the formation of HCO_3^- probably originates from either $HCOO^-$ species or CO_3^{2-} species. When using Na_2CO_3 in Table 4, it is obvious that only CO_3^{2-} (1460 cm^{-1}) species containing the added and the dissolved parts are involved in solution before reaction. Na_2CO_3 (1460 cm^{-1}) and HCOONa (1600 and 1360 cm^{-1}) are concurrently detected out after 24 h reaction. We conclude that CO_3^{2-} should be firstly transformed into $HCOO^-$ from the above two-activity phenomenon that gradual transformation of Na_2CO_3 into HCOONa gives the rising activity and $NaHCO_3$ presents the low activity. Furthermore, the $NaHCO_3$ (1310 cm^{-1}) in Fig. 6(b) should be generated due to the transformation of $HCOO^-$. As a result, this implements the transformation of CO_3^{2-} to HCO_3^- via $HCOO^-$. Similar phenomenon was also observed by Zhao et al. [42] that HCO_3^- and $HCOO^-$

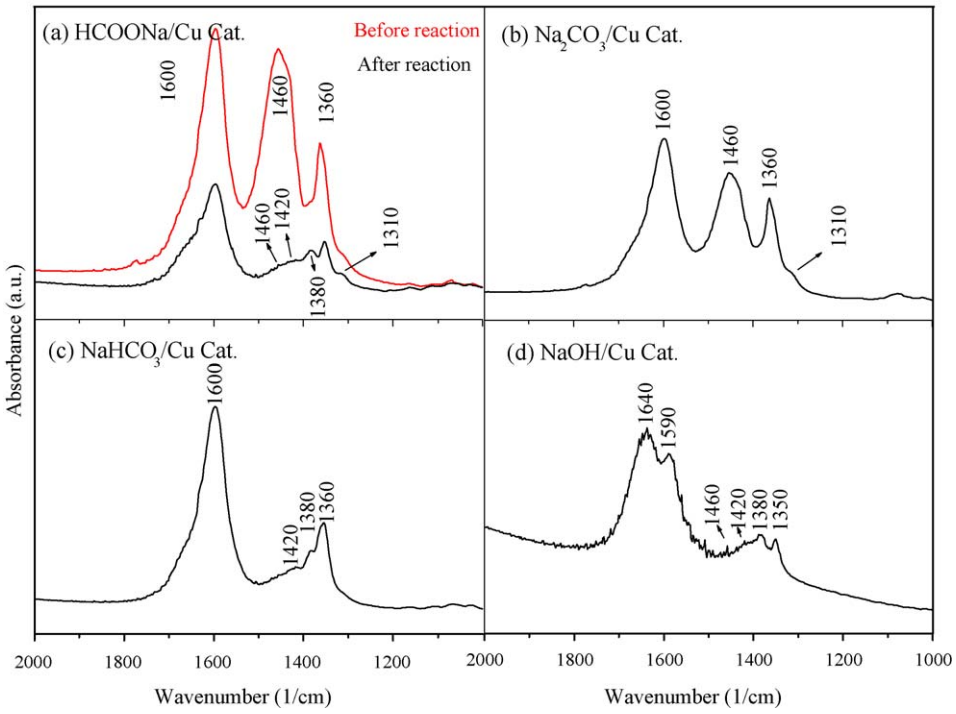

Fig. 6. FT-IR spectra for the soluble Na components in liquid phase before and after reactions over the Cu/MgO–Na catalyst: (a) Before and after reactions of HCOONa/(Cu/MgO–Na); after reactions of (b) Na_2CO_3/(Cu/MgO–Na), (c) $NaHCO_3$/(Cu/MgO–Na) and (d) NaOH/(Cu/MgO–Na).

were emerged during the synthesis reaction of ethyl formate at low temperatures from $CO/CO_2/H_2$ in the presence of K_2CO_3 and methanol solvent from ^{13}CNMR spectra.

When using $NaHCO_3$ in Table 4, $NaHCO_3$ (1420 cm^{-1}), HCOONa (1600 and 1360 cm^{-1}) and CH_3ONa (1380 cm^{-1}) are detected out after reaction. Since $HCOO^-$ might also come from CO_3^{2-} according to above results, the source of $HCOO^-$ has three possibilities: (1) the dissolved CO_3^{2-} from the Cu/MgO–Na is transformed into $HCOO^-$; (2) HCO_3^- can also be directly transformed into $HCOO^-$; (3) HCO_3^- is preferentially transformed into CO_3^{2-} and then CO_3^{2-} changes to $HCOO^-$. The third one is excluded by the reaction data that $NaHCO_3$ does not show similar activity with Na_2CO_3 as shown in Fig. 5. Also, the relative ratio of peak intensities of $HCOO^-$ to HCO_3^- is obviously larger in Fig. 6(c) than in Fig. 6(a) after reaction, thus it is suggested that HCO_3^- be consumed and $HCOO^-$ be formed simultaneously through the former two ways. This is also supported by the experimental fact that $NaHCO_3$ enhances the activity to a small extent compared to that in the absence of alkali compound in Fig. 5. Virtually, the HCO_3^- species could be hydrogenolyzed to formate species according to the report by Yang et al. [39].

When using NaOH in Fig. 6(d), HCOONa (1590 and 1350 cm^{-1}) and $NaHCO_3$ (1640 and 1420 cm^{-1}) are observed after reaction, the FT-IR spectra is similar to that in the case of HCOONa. It is in agreement with the actual reaction data that HCOONa and NaOH have the similar reaction performances after a short reaction period. It is believed that the active NaOH can react with CO to produce HCOONa, as is an industrial route of HCOONa manufacture.

As to the formation of CH_3ONa, our previous data [25] proved the existence of adsorbed NaOH on the surface of solid copper catalyst in the reaction system HCOONa/(Cu/MgO–Na), so the appearance of HCOONa should be accompanied with CH_3ONa by a conventional reaction of $NaOH + CH_3OH = CH_3ONa + H_2O$. Therefore, the transformation pathways of Na compounds can be interpreted in the following chart (5). This explains why the HCOONa and CH_3ONa almost exist in all cases. These pathways represent the possible transferring routes in the reaction systems of alkali-promoted methanol synthesis in liquid phase. More importantly, the present HCOONa/(Cu/MgO–Na) shows quite different catalytic behavior from the CH_3ONa/(Cu/MgO–Na) which had rapidly decreasing CO conversion with the reaction time [25], we hence propose that formate be the essential species for the LTMS in alcohol solvent according to the above reaction data as well as the result that alkyl formates were the intermediates [25]. This result argues against Palekar's report [8] where the active methoxide was the active site, confirming that our reaction system follows some novel catalytic routes and reaction mechanisms for the inter-transformations of these species.

Table 4
Analysis results of FT-IR spectra for various soluble Na components in liquid phase before and after reactions over Cu/MgO–Na catalyst.

Catalyst systems	Original species before reaction	FT-IR analysis after reaction	
		Observable bands (cm^{-1})[a]	Attributions
HCOONa/(Cu/MgO–Na)	Na_2CO_3 HCOONa	1600, 1360 1420, 1310 1380	HCOONa $NaHCO_3$ CH_3ONa
Na_2CO_3/(Cu/MgO–Na)	Na_2CO_3	1600, 1360 1460 1310	HCOONa Na_2CO_3 $NaHCO_3$
$NaHCO_3$/(Cu/MgO–Na)	Na_2CO_3 $NaHCO_3$	1600, 1360 1420 1380	HCOONa $NaHCO_3$ CH_3ONa
NaOH/(Cu/MgO–Na)	Na_2CO_3 NaOH	1590, 1350 1640, 1420, 1460 1380	HCOONa $NaHCO_3$ CH_3ONa

[a] The bands are recorded from Fig. 6.

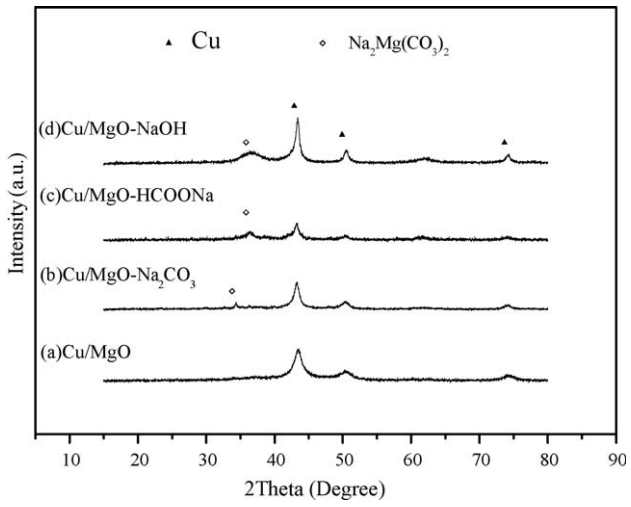

Fig. 7. XRD patterns for the used Cu/MgO–Na catalysts with different soluble Na compounds as promoters: (a) HCOONa, (b) Na_2CO_3, (c) $NaHCO_3$ and (d) NaOH.

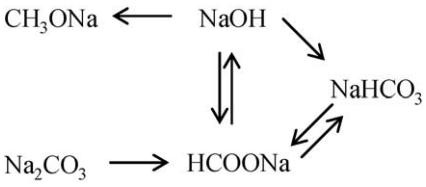

(5)

3.2.3. XRD patterns of used Cu/MgO–Na catalyst

XRD patterns of the used Cu/MgO–Na catalysts are investigated in Fig. 7. In all the cases, peaks of Cu metal phase are remained; whereas, the phase of $Na_2Mg(CO_3)_2$ grows sharper compared to that before use in Fig. 1(b); the phases of other Na compounds are not seen. In the case of Na_2CO_3 shown in Fig. 7(b), Cu peaks become quite weak, which verifies that the Cu phase might transfer its crystalline structure through some strong interaction between solid Cu/MgO catalyst and Na_2CO_3 in the alcohol solvent. This may be one of reasons that Na_2CO_3 impregnation provides the Cu/MgO precursor with activity at the largest profit.

3.3. Consumption of Na dopants

Although the present catalyst exhibits the quite high early activity and satisfactory methanol selectivity, the activity experiences a serious drop after approximately 6 h reaction. First of all, the re-addition experiments of ethanol solvent and HCOONa are carried out after 14 h absolute drop of activity, as shown in Fig. 8. One can see that the re-addition of ethanol does not regenerate the activity, so the change of solvent composition is not responsible for the drop of activity. However, CO conversion is recovered to 70% of initial activity with the re-addition of HCOONa. The fact demonstrates that Cu/MgO–Na catalyst still keeps high hydrogenolysis activity after the activity drop, and thus surface chemistry change or sintering of copper catalyst should be not the main reason for this drop of activity. Alternatively, the consumption of active HCOONa to low active $NaHCO_3$ proved by above FT-IR analysis in liquid phase is contributable to the activity drop.

Subsequently, we will hinder the consumption of HCOONa for maintaining high activity through tuning the composition of feed gas. CO/H_2 (1:1) and CO_2-containing $CO/2H_2$ are separately appended as feed gases under same reaction conditions, Fig. 9 shows the plots of CO conversions. One can see that for CO/H_2, CO

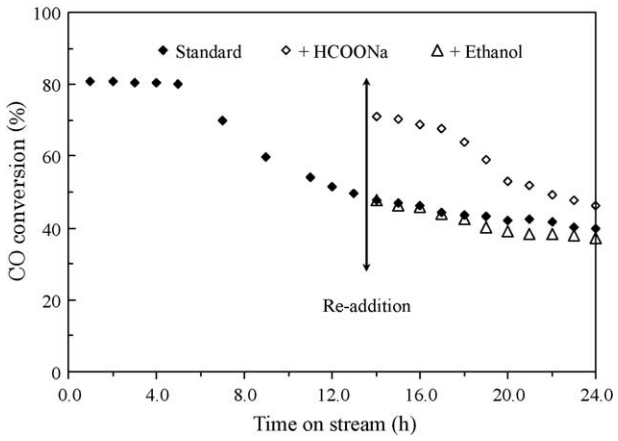

Fig. 8. Effects of re-addions of ethanol solvent and HCOONa on syngas conversions. Initial conditions: Cu/MgO–Na catalyst, 2 g; HCOONa, 10 mmol; syngas flowrate, 90 ml/min; 433 K, 5.0 MPa. Re-addition: after 14 h reaction, ethanol, 10 ml; HCOONa, 10 mmol.

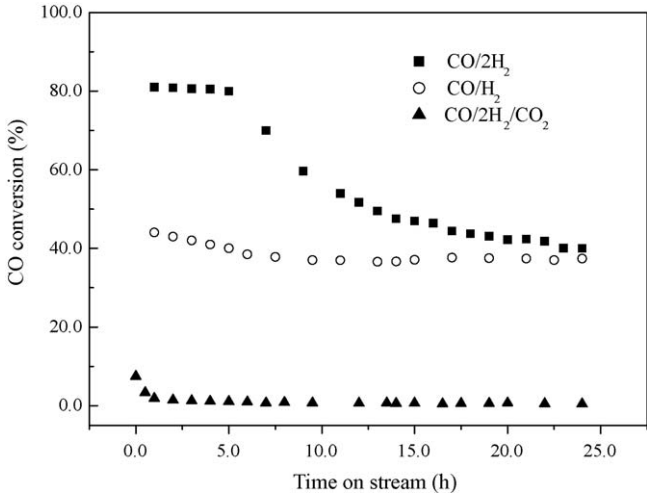

Fig. 9. Effect of different feed gases on catalytic activities of HCOONa/(Cu/MgO–Na) catalyst system. Reaction conditions: HCOONa, 10 mmol; Cu/MgO–Na catalyst, 2 g; feedgas flowrate, 90 ml/min; ethanol, 30 ml; 433 K, 5.0 MPa.

conversion almost keeps a stable and considerable level for long hours; in another way, rate of CO consumption is 1.5 times at steady state (24 reaction hours) more than that in case of $CO/2H_2$, revealing that the CO turnover rate of present catalyst is quite highly active. Additionally, even 1% CO_2 which is contained in feed syngas decreases the activity so markedly that CO_2 probably participates in the consumption process of HCOONa according to the above results. The transformation route of HCOONa into $NaHCO_3$ is proposed as the following Eq. (6):

$$HCOONa + CO_2 \rightarrow NaHCO_3 + CO \qquad K_{1p} \tag{6}$$

According to thermodynamic calculation by a MALT software (Kagaku Gijutsu-Sha, Japan), in Eq. (6), equilibrium conversion of HCOONa is 17.40% with K_{1p} = 1.23E−01 under standard reaction conditions of 433 K and 5.0 MPa, donating the feasibility of this reaction. Therefore, it is logical that the supplement CO beyond the conventional stoimetric ratio of 1/2 inhibits the consumption of HCOONa into $NaHCO_3$; however, CO_2 which is detected as a product listed in Table 1 accelerates this process. It is also noted that although H_2O is not analyzed, it is probably formed during

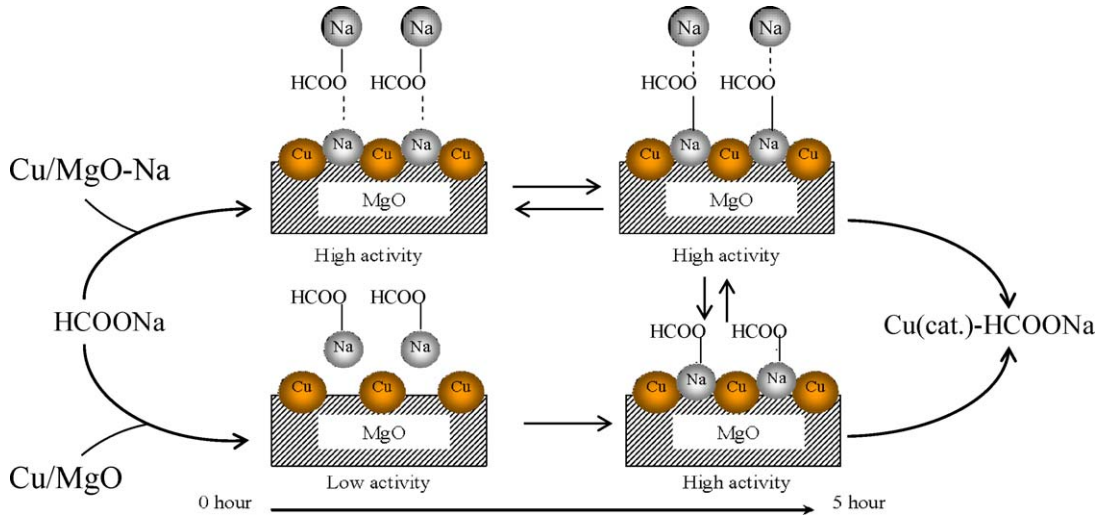

Scheme 1. Schematic for the formation of active site over Cu/MgO and Cu/MgO–Na catalysts.

reaction, because a trace of DME (not shown here) that is produced through the dehydration of methanol is repeatedly checked [10].

4. Discussions

Based on the above results, in the present low temperature process of methanol synthesis via alkyl formate, because the carbonylation of alcohol was rate-limiting step and the hydrogenolysis ability of Cu/MgO catalyst to alkyl formate was very rapid [24], we suggest that the impregnation of Na dopant strengthen the interaction of solid Cu/MgO with soluble HCOONa to form active site [25] and activate Cu/MgO catalyst through shortening the induction period of active species formation. Additionally, although the soluble Na_2CO_3 in ethanol solvent can convert into HCOONa, Cu/MgO–Na in the absence of soluble Na compounds remains a low and stable CO conversion as the proceeding of reaction shown in Fig. 5, which deduces that the most part of impregnated Na_2CO_3 in the Cu/MgO–Na is not converted into HCOONa. This phenomenon indicates that the impregnated CO_3^{2-} with Cu/MgO precursor is inactive, and thus does not constitute the active site. Furthermore, the above experiment results that formate is a key species, clarify vigorously that the real active site is the complex of soluble HCOONa, not other species (like CO_3^{2-}, OH^- and HCO_3^-), with solid copper catalyst [25]. Because the formate or hydroxide phases are absent from the resultant Cu/MgO–HCOONa and Cu/MgO–NaOH catalysts, the efforts to impregnate HCOONa or NaOH into Cu/MgO for attaining the expectably stable Cu-formate active species without undergoing the by-pass reactions have made lower active catalysts compared to Cu/MgO–Na catalyst. However, the acquired knowledge highlight one strategy on how to determine an active site and further to contrive the realistic active site in succeeding a promising catalyst system.

Some further work is needed to clarify the working behaviors of alkali dopants more specifically, we barely imagine Scheme 1 to explain the activity difference between Cu/MgO and Cu/MgO–Na since some reversible interaction between soluble alkali formate and solid copper catalysts (Cu/MgO and Cu/MgO–Na) has already been evidenced [25]. For Cu/MgO–Na, the high early activity suggests that Na dopant on surface of Cu/MgO–Na speeds up the combination with formate in solvent to form active site (Cu–Na···HCOO); for Cu/MgO reduced at higher temperature of 623 K, the surface of solid catalyst chemically adsorbs soluble HCOONa to accomplish ultimate formation of active site, which is slower than that in the presence of Na, thus exhibiting a gradually increasing activity with an induction period. Therefore, it is logical to stress that the required Cu–Na interaction sites are more easily formed if Na dopant has already existed at the catalyst surface. Once the active site is successfully produced, the formation of alkyl formates (MeF and EtF) through its reacting with ethanol and their subsequent hydrogenolysis to synthesize the methanol by activated H–Cu will be followed to finish the catalytic circle [25].

Some groups have advised that HCOO–Cu be an active centre of Cu-based catalyst for alkali-free LTMS in alcohol solvent, but activity was relatively low [38,39]. Therewithal, we propose that the presence of Na dopant contributing to the catalysis centre (Cu···Na–HCOO) with higher activity than HCOO–Cu should be the essence of alkali promotion in LTMS process. Accordingly, it is strongly recommend that the carbonylation step of alcohol where ethanol react with active site to produce alkyl formates should not be a simply homogeneous process, which is well acknowledged in the alkoxide/copper catalytic system, but primarily happen at the surface of solid catalyst [25]; the solid copper catalyst fulfills binary roles in carbonylation and hydrogenolysis. It is emphasized that, at all events, existence of alkali component either in solvent or in solid catalyst is crucial for LTMS over the substantial Cu/MgO catalyst, since Cu/MgO alone gave no activity as proved previously [25].

5. Conclusions

In summary, we demonstrate the important roles played by alkali promoter in enhancing the catalytic performance of Cu/MgO catalyst for the LTMS in slurry phase yielding high conversion per pass. In the light of impregnation, Na_2CO_3 impregnation exhibits the coordination effect better than NaOH and HCOONa due mainly to chemical interaction between alkali and copper magnesium surface. The alkali impregnation behaves to improve hydrogenolysis activity of solid copper catalyst, and strengthens the interaction of solid Cu/MgO with soluble HCOONa to easily form a highly active site (Cu···Na–HCOO) through shortening the induction period of reaction. We suggest it to be the essence of alkali promotion in the LTMS process and the reason why alkali-assisted catalytic system is more active than alkali-free LTMS processes over Cu-based catalyst.

From another aspect, alkali compounds (Na_2CO_3, $NaHCO_3$ and NaOH) in ethanol solvent can be transformed into alkali formate (HCOONa) by copper magnesium catalyst, with the aid of high-pressure syngas, to exhibit the catalytic functions. Formate is the only essential species for LTMS. The pathway for the consumption

of HCOONa into inactive $NaHCO_3$ is responsible for rapid activity drop after several hours on stream. To conquer it, we can adjust composition of feed syngas with considerations of changing the reversible dynamic equilibrium movement where HCOONa and $NaHCO_3$ work together.

Acknowledgements

The authors express the grateful appreciation on the fruitful discussions with Dr. Xingdong Yuan, Prof. Xiaohong Li and Prof. Kenji Asami.

References

[1] G.C. Chinchen, P.J. Denny, J.R. Jennings, M.S. Spencer, K.C. Waugh, Appl. Catal. 36 (1988) 1–65.
[2] H.H. Kung, Catal. Today 11 (1992) 443–453.
[3] Y. Ma, Q. Ge, W. Li, H. Xu, Appl. Catal. B: Environ. 90 (2009) 99–104.
[4] J. Toyir, P.R. Piscina, J.L.G. Fierro, N. Homs, Appl. Catal. B: Environ. 29 (2001) 207–215.
[5] Y. Amao, T. Watanabe, Appl. Catal. B: Environ. 86 (2009) 109–113.
[6] P.J.A. Tijm, F.J. Waller, D.M. Brown, Appl. Catal. A: Gen. 221 (2001) 275–282.
[7] Brookhaven National Laboratory, US Patent, 4,935,395 (1990).
[8] V.M. Palekar, H. Jung, J.W. Tierney, I. Wender, Appl. Catal. 103 (1993) 105–122.
[9] Z. Liu, J.W. Tierney, Y.T. Shah, I. Wender, Fuel Process. Technol. 23 (1989) 149–167.
[10] S. Ohyama, Appl. Catal. A: Gen. 180 (1999) 217–225.
[11] E.S. Lee, K. Aika, J. Mol. Catal. 141 (1999) 241–248.
[12] M. Marchionna, M.D. Girolamo, L. Tagliabue, M.J. Spangler, T.H. Fleiach, Stud. Surf. Sci. Catal. 119 (1998) 539–544.
[13] N. Tsubaki, J.Q. Zeng, Y. Yoneyama, K. Fujimoto, Catal. Commun. 2 (2001) 213–217.
[14] L. Fan, Y. Sakaiya, K. Fujimoto, Appl. Catal. A: Gen. 180 (1999) L11–L13.
[15] N. Tsubaki, M. Ito, K. Fujimoto, J. Catal. 197 (2001) 224–227.
[16] J.Q. Zeng, K. Fujimoto, N. Tsubaki, Energy Fuels 160 (2002) 83–86.
[17] H.N. Evin, G. Jacobs, G.A. Thomas, B.H. Davis, Catal. Lett. 120 (2008) 166–178.
[18] T. Fukunaga, V. Ponec, Appl. Catal. A: Gen. 154 (1997) 207–219.
[19] G. Larsen, G.L. Haller, Catal. Lett. 3 (1989) 103–110.
[20] K. Klier, Catal. Today 15 (1992) 361–382.
[21] G.R. Sheffer, T.S. King, J. Catal. 115 (1989) 376–387.
[22] G.R. Sheffer, T.S. King, J. Catal. 116 (1989) 488–497.
[23] B. Hu, K. Fujimoto, Appl. Catal. A: Gen. 346 (2008) 174–178.
[24] B. Hu, K. Fujimoto, Catal. Lett. 129 (2009) 416–421.
[25] B. Hu, Y. Yamaguchi, K. Fujimoto, Catal. Commun. 10 (2009) 1620–1624.
[26] J.M. Campbell, J. Nakamura, C.T. Campbell, J. Catal. 136 (1992) 24–42.
[27] A. Pabst, Am. Mineral. 58 (1973) 211–217.
[28] Y. Zhang, Y.H. Sun, B. Zhong, J. Fuel Chem. Technol. (Chin.) 30 (2002) 277–280.
[29] Z. Liu, J.W. Tierney, Y.T. Shan, I. Wender, Fuel Process. Technol. 18 (1988) 185–189.
[30] L.H. Huang, W. Chu, Y. Long, Z.M. Ci, S.Z. Luo, Catal. Lett. 108 (2006) 113–118.
[31] D.M. Monti, M.A. Kohler, M.S. Wainwright, D.L. Trimm, N.W. Cant, Appl. Catal. A: Gen. 22 (1986) 123–136.
[32] M.W.E. Van den Berg, S. Polarz, O.P. Tkachenko, K.V. Klementiev, M. Bandyopadhyay, L. Khodeir, H. Gies, M. Muhler, W. Grünert, J. Catal. 241 (2006) 446–455.
[33] H. Wilmer, O. Hinrichsen, Catal. Lett. 82 (2002) 117–122.
[34] M. Kurtz, N. Bauer, C. Büscher, H. Wilmer, O. Hinrichen, R. Becker, S. Rabe, K. Merz, M. Driess, R.A. Fischer, M. Muhler, Catal. Lett. 92 (2004) 49–52.
[35] I. Nakamura, T. Fujitani, T. Watanabe, T. Uchijima, J. Nakamura, Catal. Lett. 35 (1995) 297–302.
[36] W.P.A. Jansen, J. Beckers, J.C. Van der Heuvel, A.W.D. Van der Gon, A. Bliek, H.H. Brongersma, J. Catal. 210 (2002) 229–236.
[37] M.M. Günter, T. Ressler, R.E. Jentoft, B. Bems, J. Catal. 203 (2001) 133–149.
[38] Y. Zhang, R.Q. Yang, N. Tsubaki, Catal. Today 132 (2008) 93–100.
[39] R.Q. Yang, Y. Zhang, I. Yuki, N. Tsubaki, Appl. Catal. A: Gen. 288 (2005) 126–133.
[40] R.Q. Yang, Y. Fu, Y. Zhang, N. Tsubaki, J. Catal. 228 (2004) 23–35.
[41] S. Fujita, S. Moribe, Y. Kanamori, M. Kakudate, N. Takezawa, Appl. Catal. A: Gen. 207 (2001) 121–128.
[42] T.S. Zhao, Y. Yoshiharu, K. Fujimoto, N. Yamane, K. Fujimoto, N. Tsubaki, Chem. Lett. 36 (2006) 734–735.